Vibrational Analysis of Peptides, Polypeptides, and Proteins. XI. β-Poly(L-alanine) and Its N-Deuterated Derivative

Anil M. Dwivedi and S. Krimm*

Biophysics Research Division, The University of Michigan, Ann Arbor, Michigan 48109.
Received June 3, 1981

ABSTRACT: The infrared spectrum of N-deuterated β-poly(L-alanine) has been obtained and used, together with an improved transferable force field for poly(glycine I),[1] to make a significant improvement in the force field and band assignments of β-poly(L-alanine). Assignment of the unperturbed ND stretch frequency confirms our previous analysis indicating that the hydrogen bond in this antiparallel-chain pleated-sheet structure is stronger than that in the antiparallel-chain rippled-sheet structure of poly(glycine I).

Introduction

In order to develop a force field with maximum transferability for peptide molecules, we recently[1] rerefined the force field for poly(glycine I) [$(Gly\ I)_n$] in the antiparallel-chain rippled-sheet (APRS) structure. In doing so we were also able to improve its prediction of certain CH_2 modes and to show that it accounted satisfactorily for the frequencies of four isotopic species of this molecule.

During this refinement we optimized the force field for transferability to β-poly(L-alanine) [β-$(Ala)_n$], which has an antiparallel-chain pleated-sheet (APPS) structure. Although we have presented a detailed vibrational analysis of this molecule,[2] there are a number of motivations to reexamine its force field. First, we wish to incorporate changes that are indicated by the $(Gly\ I)_n$ rerefinement and to examine the force field transferability. Second, we have prepared N-deuterated β-$(Ala)_n$, and as with $(Gly\ I)_n$, this can serve as an additional check on the force field. In fact, this has led to some modifications of previous assignments.[2] Third, we have used this occasion to improve the prediction of some of the CH_3 modes. And finally, an optimized force field for β-$(Ala)_n$ provides the soundest basis for refining an "approximate" force field[3] (in which CH_3 is represented by a point mass) that can be more realistically applied to the calculation of the normal modes of large molecules such as globular proteins.

Experimental Section

Infrared spectra of $(Ala)_n$ (Sigma, no. P-5517, type II, lot 77C-5006, M = 15000) in KBr disks confirmed that this sample was in the β conformation. When the disks were dissolved in trifluoroacetic acid and the $(Ala)_n$ was precipitated from acid solution by anhydrous ether and dried in vacuo, the spectrum showed that very little change in conformation occurred. We therefore deuterated the sample by using the same procedure with deuterated trifluoroacetic acid (Sigma, T3136, 99% D). The spectrum, obtained on a Perkin-Elmer Model 180, is shown in Figure 1. (Some bands of CF_3COO^- are observed in the KBr pellet spectrum.) A sample was also treated by heating in D_2O several times, but its level of deuteration was lower than that of the above sample; it served, however, to check various deuterated bands. Raman spectra could not be obtained because of the very high fluorescence of this sample.

Normal Mode Calculation

As in the previous study,[2] the general chain and sheet structures used in the normal mode calculation are those of Arnott et al.[4] The structural parameters of the peptide unit are the same as those we used earlier,[2] as is the setting angle α (80°) that specifies the orientation of a chain with respect to the sheet. The exact dihedral angles are ϕ = −138.38° and ψ = 135.73°. We have taken the rotation angle about C^α–C^β to be χ = 57.5°, in accordance with the results of conformational energy calculation.[5] The axial shift between adjacent chains in the same sheet is taken from amide I band splittings,[6] which arise from transition dipole coupling;[7,8] its value is −0.27 Å. The unit cell dimensions are the same as those used previously[2] and lead to the following exact sheet parameters: r(H···O) = 1.754 Å, r(N···O) = 2.731 Å, $r(H^\alpha \cdots H^\alpha)$ = 2.325 Å, θ(N–H,NO) = 9.84°, γ(N–H···O) = 164.57°. In order to maintain transferability of force constants the peptide group is kept planar.

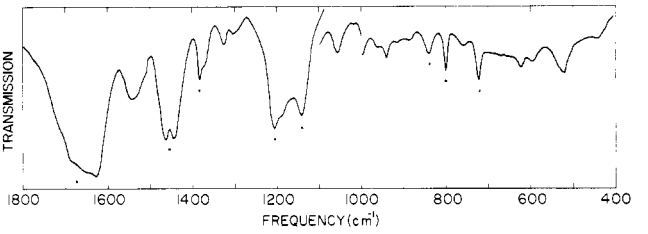

Figure 1. Infrared spectrum of β-poly(L-alanine-*N*-*d*), deuterated with trifluoroacetic acid-*O*-*d* and examined in a KBr pellet. Bands designated with asterisks are positions of strong CF_3COO^- bands.[16]

The APPS structure belongs to the D_2 point group, whose symmetry species show the following distribution of normal modes and activity: $A[\nu(0,0)^6]$-30, Raman; B_1-$[\nu(0,\pi)]$-29 Raman, infrared (∥); $B_2[\nu(\pi,0)]$-29, Raman, infrared (⊥); $B_3[\nu(\pi,\pi)]$-29, Raman, infrared (⊥). The internal and local symmetry coordinates of one chemical repeat unit are the same in the present calculation as used in the earlier work.[2] The symmetry coordinates for each species are also obtained from the appropriate combinations of local symmetry coordinates, which were presented in an earlier paper.[6]

The force field refinement was accomplished in two stages. First, three subsets of variable force constants were chosen to be used in the least-squares refinement program, and these were adjusted to give the best possible fit to the experimental infrared and Raman data. The force field thus obtained gave quite satisfactory agreement for the N-deuterated molecule. Second, the force field was reviewed with respect to that for $(Gly\ I)_n$,[1] and some minor changes were made manually in order to improve transferability of force constants; this had no significant effect on the frequency agreement. A complete list of the force constants is given in Table I. Dispersions in additionally refined force constants in the range of 0.1–0.8 averaged about 6%. Some features of this force field, in comparison to that of $(Gly\ I)_n$, will be discussed later.

0024-9297/82/2215-0186$01.25/0 © 1982 American Chemical Society

Table I
Force Constants for β-Poly(L-alanine)

force constant[a]	value[b]	force constant	value
1. $f(NC^{\alpha})$	4.523	54. $f(C^{\alpha}C,C^{\alpha}CO)$	0.200
2. $f(C^{\alpha}C)$	4.160	55. $f(C^{\alpha}C,NC^{\alpha}H^{\alpha})$	0.026
3. $f(CN)$	6.415	56. $f(C^{\alpha}C,CC^{\alpha}H^{\alpha})$	0.205
4. $f(CO)$	9.882	57. $f(C^{\alpha}C,CC^{\alpha}C^{\beta})$	0.367
5. $f(NH)$	5.674	58. $f(C^{\alpha}C,H^{\alpha}C^{\alpha}C^{\beta})$	0.079
6. $f(C^{\alpha}H^{\alpha})$	4.4628	59. $f(CN,C^{\alpha}CN)$	0.300
7. $f(C^{\alpha}C^{\beta})$	4.980	60. $f(CN,CNC^{\alpha})$	0.300
8. $f(C^{\beta}H^{\beta})$	4.800	61. $f(CN,NCO)$	0.200
9. $f(H\cdots O)$	0.150	62. $f(CN,CNH)$	0.294
10. $f(H^{\alpha}\cdots H^{\alpha})$	0.0027	63. $f(CO,C^{\alpha}CO)$	0.450
11. $f(NC^{\alpha}C)$	0.819	64. $f(CO,NCO)$	0.450
12. $f(C^{\alpha}CN)$	1.033	65. $f(C^{\alpha}C^{\beta},NC^{\alpha}H^{\alpha})$	0.079
13. $f(CNC^{\alpha})$	0.5259	66. $f(C^{\alpha}C^{\beta},NC^{\alpha}C^{\beta})$	0.617
14. $f(NCO)$	1.246	67. $f(C^{\alpha}C^{\beta},CC^{\alpha}H^{\alpha})$	0.079
15. $f(NC^{\alpha}H^{\alpha})$	0.765	68. $f(C^{\alpha}C^{\beta},CC^{\alpha}C^{\beta})$	0.417
16. $f(NC^{\alpha}C^{\beta})$	1.193	69. $f(C^{\alpha}C^{\beta},H^{\alpha}C^{\alpha}C^{\beta})$	0.415
17. $f(C^{\alpha}NH)$	0.527	70. $f(C^{\alpha}C^{\beta},C^{\alpha}C^{\beta}H)$	0.353
18. $f(C^{\alpha}CO)$	1.246	71. $f(NC^{\alpha}C,C^{\alpha}NH)$	−0.100
19. $f(CC^{\alpha}H^{\alpha})$	0.684	72. $f(NC^{\alpha}C,NC^{\alpha}H^{\alpha})$	−0.031
20. $f(CC^{\alpha}C^{\beta})$	1.181	73. $f(NC^{\alpha}C,CC^{\alpha}C^{\beta})$	−0.041
21. $f(CNH)$	0.527	74. $f(NC^{\alpha}C,NC^{\alpha}C^{\beta})$	0.200
22. $f(H^{\alpha}C^{\alpha}C^{\beta})$	0.5175	75. $f(NC^{\alpha}C,CO\ ob)$	−0.0725
23. $f(C^{\alpha}C^{\beta}H)$	0.677	76. $f(NC^{\alpha}C,NH\ ob)$	0.110
24. $f(HC^{\beta}H)$	0.524	77. $f(C^{\alpha}CN,CNH)$	0.200
25. $f(CO\cdots H\ ib)$	0.010	78. $f(CNC^{\alpha},NC^{\alpha}H^{\alpha})$	0.100
26. $f(NH\cdots O\ ib)$	0.056	79. $f(NC^{\alpha}H^{\alpha},CC^{\alpha}H^{\alpha})$	0.019
27. $f(CO\ ob)$	0.587	80. $f(NC^{\alpha}H^{\alpha},H^{\alpha}C^{\alpha}C^{\beta})$	0.043
28. $f(NH\ ob)$	0.129	81. $f(NC^{\alpha}H^{\alpha},NH\ ob)$	0.1022
29. $f(NC^{\alpha}\ t)$	0.037	82. $f(NC^{\alpha}C^{\beta},CC^{\alpha}C^{\beta})$	−0.041
30. $f(C^{\alpha}C\ t)$	0.037	83. $f(NC^{\alpha}C^{\beta},H^{\alpha}C^{\alpha}C^{\beta})$	−0.031
31. $f(CN\ t)$	0.680	84. $f(NC^{\alpha}C^{\beta},C^{\alpha}C^{\beta}H)_T$	−0.049
32. $f(NH\ t)$	0.0015	85. $f(NC^{\alpha}C^{\beta},C^{\alpha}C^{\beta}H)_G$	0.040
33. $f(CO\ t)$	0.001	86. $f(NC^{\alpha}C^{\beta},NH\ ob)$	0.120
34. $f(C^{\alpha}C^{\beta}\ t)$	0.110	87. $f(C^{\alpha}CO,CC^{\alpha}H^{\alpha})$	0.150
35. $f(NC^{\alpha},C^{\alpha}C)$	0.300	88. $f(NCO,CNH)$	0.251
36. $f(C^{\alpha}C,CN)$	0.300	89. $f(C^{\alpha}NH,CNH)$	0.038
37. $f(CN,NC^{\alpha})$	0.300	90. $f(C^{\alpha}NH,NC^{\alpha}H^{\alpha})$	0.100
38. $f(NC^{\alpha},C^{\alpha}C^{\beta})$	0.101	91. $f(CC^{\alpha}H^{\alpha},CO\ ob)$	0.150
39. $f(C^{\alpha}C,C^{\alpha}C^{\beta})$	0.101	92. $f(CC^{\alpha}C^{\beta},H^{\alpha}C^{\alpha}C^{\beta})$	−0.031
40. $f(C^{\alpha}C,CO)$	0.500	93. $f(CC^{\alpha}C^{\beta},CO\ ob)$	0.162
41. $f(CN,CO)$	0.500	94. $f(C^{\alpha}C^{\beta}H,C^{\alpha}C^{\beta}H)$	−0.045
42. $f(C^{\beta}H,C^{\beta}H)$	0.071	95. $f(C^{\alpha}C^{\beta}H,H^{\alpha}C^{\alpha}C^{\beta})_T$	0.122
43. $f(C^{\alpha}H^{\alpha},H^{\alpha}\cdots H^{\alpha})$	−0.0075	96. $f(C^{\alpha}C^{\beta}H,H^{\alpha}C^{\alpha}C^{\beta})_G$	0.100
44. $f(NC^{\alpha},CNC^{\alpha})$	0.300	97. $f(CO\ ob,NH\ ob)$	0.010
45. $f(NC^{\alpha},NC^{\alpha}C)$	0.300	98. $f(NH\cdots O\ ib,NH\ ob)$	−0.039
46. $f(NC^{\alpha},C^{\alpha}NH)$	0.294	99. $f(CO\ ob,CN\ t)$	0.0111
47. $f(NC^{\alpha},NC^{\alpha}H^{\alpha})$	0.627	100. $f(NH\ ob,CN\ t)$	−0.1477
48. $f(NC^{\alpha},NC^{\alpha}C^{\beta})$	0.417	101. $F_{10,I}$	0.120
49. $f(NC^{\alpha},CC^{\alpha}H^{\alpha})$	0.026	102. $F_{01,I}$	−0.347
50. $f(NC^{\alpha},H^{\alpha}C^{\alpha}C^{\beta})$	0.079	103. $F_{11,I}$	0.160
51. $f(NC^{\alpha},CC^{\alpha}C^{\beta})$	0.200	104. $F_{10,II}$	−0.027
52. $f(C^{\alpha}C,NC^{\alpha}C)$	0.300	105. $F_{01,II}$	−0.004
53. $f(C^{\alpha}C,C^{\alpha}CN)$	0.300	106. $F_{11,II}$	0.014

[a] $f(AB)$ = AB bond stretch, $f(ABC)$ = ABC angle bend, $f(X,Y)$ = XY interaction, F = transition dipole coupling;[7] ib = in-plane bend, ob = out-of-plane bend, t = torsion, T = trans, G = gauche. [b] Units are mdyn/Å for stretch and stretch,stretch force constants, mdyn for stretch,bend force constants, and mdyn·Å for all others.

Results and Discussion

The observed and calculated frequencies of APPS $(Ala)_n$ and its N-deuterated derivative are given in Table II. Raman data are from Fanconi[9] and Frushour and Koenig.[10] For the infrared bands, we have used our observed frequencies in the 3300–400-cm^{-1} region and the dichroic and far-infrared data of Elliott[11] and Itoh et al.[12] Our infrared spectra indicate that some disordered material is present, particularly by the presence of significant amide I absorption[13] near 1660 cm^{-1}. This has led us also to assign the 1240-cm^{-1} infrared band to a disordered component,[13] revising our earlier assignment[2] of this band to the APPS structure. (Careful examination of polarized spectra[11,12] shows that this band in fact exhibits practically no dichroism.) Band assignments have been made on the basis of the following considerations: (a) bands appearing only in the Raman spectrum are assigned to the A species; (b) infrared bands of parallel dichroism are assigned to the B_1 species; (c) infrared bands of perpendicular dichroism are assigned to the B_2 or B_3 species according to whether the transition moment in a chemical unit is clearly within or perpendicular to the sheet (if this direction is not obvious, we have left the exact assignment open); (d) general frequency agreement should be optimal.

The overall agreement between observed and calculated frequencies of β-$(Ala)_n$ is slightly better than in the previous calculation,[2] but what is more significant is that we have improved some assignments as a result of having the spectrum of the N-deuterated molecule. The amide I

Table II
Observed and Calculated Frequencies (in cm^{-1}) of β-Poly(L-alanine)

observed[a]		calculated				
Raman	IR	A	B_1	B_2	B_3	potential energy distribution[b]
				-(NHCH(CH_3)CO)-$_n$		
		3242				NH s (97)
			3242			NH s (97)
	3242 S[c]			3242		NH s (97)
					3242	NH s (97)
2984 S		2984				CH_3 as2 (54), CH_3 as1 (45)
	2983 M ∥		2984			CH_3 as2 (52), CH_3 as1 (47)
				2984		CH_3 as2 (55), CH_3 as1 (44)
					2984	CH_3 as2 (52), CH_3 as1 (48)
		2983				CH_3 as1 (54), CH_3 as2 (45)
			2983			CH_3 as1 (52), CH_3 as2 (47)
	2980 sh ⊥[d]			2983		CH_3 as1 (55), CH_3 as2 (44)
					2983	CH_3 as1 (52), CH_3 as2 (48)
		2929				CH_3 ss (100)
			2929			CH_3 ss (100)
				2929		CH_3 ss (100)
2933 S	2934 W ⊥				2929	CH_3 ss (100)
2871 sh		2877				$C^\alpha H^\alpha$ s (98)
					2877	$C^\alpha H^\alpha$ s (98)
			2866			$C^\alpha H^\alpha$ s (99)
	2874 VW ⊥			2866		$C^\alpha H^\alpha$ s (99)
					1695	CO s (78), CN s (13)
	1694 W ∥		1692			CO s (76), CN s (19)
1669 S		1667				CO s (73), CN s (21)
				1627		CO s (70), CN s (22)
					1593	NH ib (55), CN s (19)
1553 VW	1555 MW ⊥			1559		NH ib (52), CN s (14), $C^\alpha C$ s (13)
1538 W		1533				NH ib (49), CN s (21), CO ib (10), $C^\alpha C$ s (10)
	1524 S ∥		1525			NH ib (41), CN s (25), CO ib (12), $C^\alpha C$ s (12)
1451 S		1455				CH_3 ab1 (42), CH_3 ab2 (40)
	1454 S ∥		1455			CH_3 ab1 (45), CH_3 ab2 (38)
					1453	CH_3 ab1 (88), CH_3 r1 (10)
	1446 S ⊥			1452		CH_3 ab1 (87), CH_3 r1 (10)
1451 S		1452				CH_3 ab1 (45), CH_3 ab2 (44)
	1454 S ∥		1452			CH_3 ab2 (46), CH_3 ab1 (42)
	1446 S ⊥			1451		CH_3 ab2 (87), CH_3 r2 (10)
					1451	CH_3 ab2 (89), CH_3 r2 (10)
1399 W		1406				H^α b2 (33), $C^\alpha C$ s (16), CH_3 sb (13), NH ib (11)
	1402 MW ∥		1401			H^α b2 (36), CH_3 sb (16), $C^\alpha C$ s (13), NH ib (13)
	1386 W ⊥				1386	CH_3 sb (68), H^α b1 (17), $C^\alpha C^\beta$ s (11)
				1384		CH_3 sb (72), H^α b1 (16), $C^\alpha C^\beta$ s (11)
1368 W		1373				CH_3 sb (68), H^α b2 (12)
	1372 MW ∥		1373			CH_3 sb (65), H^α b2 (15)
1335 W	1330 W, br ⊥				1331	H^α b2 (34), NH ib (24), $C^\alpha C$ s (15), CH_3 sb (14)
				1317		H^α b2 (44), NH ib (25), $C^\alpha C$ s (12), CO s (10)
				1308		H^α b2 (24), CN s (19), CO ib (16)
1311 W	1309 sh				1307	H^α b2 (36), CN s (19), CO ib (13)
1243 S		1237				H^α b2 (37), NC^α s (19), NH ib (17), CN s (16)
1226 M	1222 S ∥		1232			H^α b2 (30), NC^α s (25), NH ib (15), CN s (13)
		1201				NC^α s (36), CH_3 r1 (14), $C^\alpha C$ s (10)
				1196		$C^\alpha C^\beta$ s (33), H^α b1 (25), NC^α s (22), CH_3 r1 (10), CH_3 sb (10)
					1197	$C^\alpha C^\beta$ s (33), H^α b1 (26), NC^α s (22), CH_3 r1 (10), CH_3 sb (10)
			1196			NC^α s (29), NH ib (13), $C^\alpha C$ s (12), H^α b2 (12), CH_3 r1 (12)
1165 W		1169				H^α b1 (58), CH_3 sb (21), $C^\alpha C^\beta$ s (12)
	1167 S ∥		1168			H^α b1 (57), CH_3 sb (20), $C^\alpha C^\beta$ s (12)
	1120 VW			1125		H^α b1 (28), CH_3 r2 (25), CH_3 sb (11)
					1125	H^α b1 (28), CH_3 r2 (26), CH_3 sb (11)
1092 S		1094				CH_3 r2 (55), $C^\alpha C^\beta$ s (22)
			1092			CH_3 r2 (54), $C^\alpha C^\beta$ s (23)
				1088		CH_3 r1 (27), CH_3 r2 (26), $C^\alpha C^\beta$ s (15), $NC^\alpha C$ d (10)
	1084 W ⊥				1088	CH_3 r2 (27), CH_3 r1 (25), $C^\alpha C^\beta$ s (13), $NC^\alpha C$ d (10)
	1052 M ⊥				1065	$C^\alpha C^\beta$ s (23), H^α b1 (21), CH_3 r1 (19), CH_3 r2 (17)
				1063		$C^\alpha C^\beta$ s (22), H^α b1 (21), CH_3 r2 (19), CH_3 r1 (17)
1065 M		1056				$C^\alpha C^\beta$ s (48), CH_3 r1 (16), H^α b1 (13)

Table II (*Continued*)

observed[a]		calculated				
Raman	IR	A	B_1	B_2	B_3	potential energy distribution[b]
			1055			$C^{\alpha}C^{\beta}$ s (46), CH_3 r1 (15), H^{α} b1 (13), CH_3 r2 (10)
967 M		969				CH_3 r1 (50), NC^{α} s (25)
	966 S ∥		969			CH_3 r1 (50), NC^{α} s (25)
909 VS		915				$C^{\alpha}C$ s (17), CH_3 r2 (16), CNC^{α} d (12), CN s (12), CO s (11)
	925 M ⊥			915		NC^{α} s (28), CH_3 r1 (24), CN s (14)
					912	NC^{α} s (30), CH_3 r1 (24), CN s (14)
	902 W ∥		906			$C^{\alpha}C$ s (17), CH_3 r2 (15), CNC^{α} d (13), CN s (13), CO s (11)
					845	$C^{\alpha}C$ s (35), NC^{α} s (13), $C^{\alpha}C^{\beta}$ s (12), CN s (11)
	837 VW					
				845		$C^{\alpha}C$ s (32), NC^{α} s (17), $C^{\alpha}C^{\beta}$ s (13)
					767	CO ib (21), NC^{α} s (16), $C^{\alpha}C$ s (14), $NC^{\alpha}C$ d (13), CNC^{α} d (11), C^{β} b2 (11)
775 M	778 MW					
				763		CO ib (20), $C^{\alpha}C$ s (17), NC^{α} s (13), $NC^{\alpha}C$ d (13), C^{β} b2 (13), CNC^{α} d (12)
				718		CN t (67), NH ob (20), NH···O t (10)
			714			CN t (39), NH ob (35), CO ob (21), H^{α} b1 (11)
	706 S ∥, ⊥					
					713	CN t (65), NH ob (18), NH···O t (10)
698 VW		710				CN t (48), NH ob (37), CO ob (15), H^{α} b1 (10), NH···O t (10)
		671				CO ob (50), CN t (28), C^{β} b1 (10)
			662			CO ob (44), CN t (41), C^{β} b1 (10)
628 VW		626				CO ib (51), $C^{\alpha}C$ s (14)
	629 W ∥		622			CO ib (54), $C^{\alpha}C$ s (14)
				623		$C^{\alpha}CN$ d (29), CO ob (29), NH ob (22), C^{β} b2 (16), CN t (13), $NC^{\alpha}C$ d (10)
	615 W ⊥					
					623	CO ob (39), NH ob (24), $C^{\alpha}CN$ d (22), C^{β} b2 (15), CN t (13)
				598		CO ob (52), $C^{\alpha}CN$ d (17)
					596	CO ob (39), $C^{\alpha}CN$ d (26)
					449	C^{β} b1 (49), NH ob (12)
	448 M ⊥			447		C^{β} b1 (51), NH ob (14)
	432 M ∥		432			C^{β} b2 (78), $NC^{\alpha}C$ d (11)
437 W		431				C^{β} b2 (77), $NC^{\alpha}C$ d (13)
	326 W ∥		327			$NC^{\alpha}C$ d (30), $C^{\alpha}C$ s (10)
332 VW		324				$NC^{\alpha}C$ d (26), C^{β} b2 (12), $C^{\alpha}C$ s (10), CO ob (10)
			289			$C^{\alpha}CN$ d (41), $C^{\alpha}C^{\beta}$ t (16), H···O s (14)
				288		CO ib (35), $NC^{\alpha}C$ d (20), CNC^{α} d (14), C^{β} b2 (16)
300 M						
					286	CO ib (34), C^{β} b2 (21), $NC^{\alpha}C$ d (18), CNC^{α} d (12), C^{β} b1 (10)
266 VW, sh		270				$C^{\alpha}CN$ d (39), $C^{\alpha}C^{\beta}$ t (28), $NC^{\alpha}C$ d (14)
				252		C^{β} b2 (51)
					250	C^{β} b2 (45)
	240 M ∥		239			$C^{\alpha}C^{\beta}$ t (70)
		238				$C^{\alpha}C^{\beta}$ t (64), $NC^{\alpha}C$ d (11)
235 M, sh				238		$C^{\alpha}C^{\beta}$ t (91)
					238	$C^{\alpha}C^{\beta}$ t (89)
			200			CNC^{α} d (45), H···O s (17), $C^{\alpha}C^{\beta}$ t (11)
185 VW		177				CNC^{α} d (65), $C^{\alpha}CN$ d (11)
					156	H···O s (61)
135 S		140				NH ob (37), CO ob (19), NC^{α} s (12), $C^{\alpha}CN$ d (10), H^{α} b2 (10)
			137			NH ob (47), CO ob (18), NC^{α} s (14), H^{α} b2 (13), $C^{\alpha}CN$ d (10)
	122 W, br			116		CNC^{α} d (22), $NC^{\alpha}C$ d (16), $C^{\alpha}CN$ d (14), NH ob (12)
			106			CN t (19), NH···O t (18), C^{β} b1 (17)
91 M, sh		91				C^{β} b1 (22), NH ob (22), H···O s (17), $C^{\alpha}C$ t (11)
					92	NH ob (29), $C^{\alpha}C$ t (21), H···O s (19), CNC^{α} d (14)
					83	CN t (39), NH···O t (17), CO···H ib (16), NH ob (14), H···O s (13), NC^{α} t (11)
				73		H···O s (30), $C^{\alpha}C$ t (27), NC^{α} t (22), CN t (14), NH ob (11)
		37				NH···O ib (39), NH···O t (32), NH ob (22), H···O s (13), CO···H t (12)
			38			NH ob (64), NH···O ib (40), CN t (20)
				30		NH···O ib (59), CN t (42), NH ob (42), CO···H ib (19)

Table II (*Continued*)

observed[a]		calculated				
Raman	IR	A	B_1	B_2	B_3	potential energy distribution[b]
		19				NH ob (37), CO···H ib (24), CO···H t (22), H^{α}···H^{α} s (19), NH···O ib (12), NH···O t (12)
				-(NDCH(CH_3)CO)-$_n$		
		2984				CH_3 as2 (51), CH_3 as1 (48)
	2986 M		2984			CH_3 as2 (54), CH_3 as1 (46)
				2984		CH_3 as2 (52), CH_3 as1 (48)
					2984	CH_3 as2 (51), CH_3 as1 (48)
		2983				CH_3 as1 (51), CH_3 as2 (48)
			2983			CH_3 as1 (54), CH_3 as2 (46)
				2983		CH_3 as1 (52), CH_3 as2 (48)
					2983	CH_3 as1 (51), CH_3 as2 (48)
		2929				CH_3 ss (100)
			2929			CH_3 ss (100)
				2929		CH_3 ss (100)
	2938 W				2929	CH_3 ss (100)
		2877				$C^{\alpha}H^{\alpha}$ s (98)
					2877	$C^{\alpha}H^{\alpha}$ s (98)
	2882 VW[e]		2866	2866		$C^{\alpha}H^{\alpha}$ s (99)
		2381				ND s (96)
			2381			ND s (96)
	~2428 S[c]			2381		ND s (96)
					2381	ND s (96)
					1689	CO s (78), CN s (17)
	1685 S		1689			CO s (76), CN s (19)
		1664				CO s (73), CN s (21)
	1628 VS			1623		CO s (69), CN s (23)
	1488 sh				1485	$C^{\alpha}C$ s (24), CN s (23), H^{α} b2 (14), CO ib (13), ND ib (12)
			1473			$C^{\alpha}C$ s (25), CN s (24), CO ib (15)
	1464 M			1471		$C^{\alpha}C$ s (22), CH_3 ab1 (15), CN s (13), CO s (11), CO ib (10), H^{α} b2 (10)
		1471				$C^{\alpha}C$ s (25), CN s (22), CO ib (14), CO s (10)
		1453	1453			CH_3 ab1 (79)
				1452		CH_3 ab2 (55), CH_3 ab1 (34)
					1452	CH_3 ab2 (54), CH_3 ab1 (35)
		1449	1449			CH_3 ab2 (73)
					1448	CH_3 ab1 (48), CH_3 ab2 (33)
	1444 S			1444		CH_3 ab1 (40), CH_3 ab2 (27)
	1384 M[e]				1380	CH_3 sb (78), H^{α} b1 (14), $C^{\alpha}C^{\beta}$ s (10)
				1380		CH_3 sb (78), H^{α} b1 (14), $C^{\alpha}C^{\beta}$ s (10)
		1378				CH_3 sb (78), H^{α} b1 (11)
	1372 M		1377			CH_3 sb (79), H^{α} b1 (10)
		1335				H^{α} b2 (77)
	1326 MW		1334			H^{α} b2 (78)
					1309	H^{α} b2 (64), CN s (12)
	1306 W			1308		H^{α} b2 (63), CN s (12)
					1208	H^{α} b1 (35), $C^{\alpha}C^{\beta}$ s (30), CH_3 sb (15), NC^{α} s (12)
	1207 S[e]			1206		H^{α} b1 (35), $C^{\alpha}C^{\beta}$ s (31), CH_3 sb (14), NC^{α} s (13)
		1200				NC^{α} s (48), CH_3 r1 (21), $C^{\alpha}C^{\beta}$ s (10)
	1190 W		1200			NC^{α} s (48), CH_3 r1 (21), $C^{\alpha}C^{\beta}$ s (10)
		1169				H^{α} b1 (56), CH_3 sb (21), $C^{\alpha}C^{\beta}$ s (12)
	1165 sh		1169			H^{α} b1 (57), CH_3 sb (21), $C^{\alpha}C^{\beta}$ s (12)
	1142 S[e]				1141	CH_3 r1 (29), NC^{α} s (14), H^{α} b1 (13), ND ib (10)
				1138		CH_3 r1 (27), H^{α} b1 (17), NC^{α} s (13)
					1111	CH_3 r2 (50), $C^{\alpha}C^{\beta}$ s (11)
				1108		CH_3 r2 (49), $C^{\alpha}C^{\beta}$ s (11), $NC^{\alpha}C$ d (10)
		1102				CH_3 r2 (50), $C^{\alpha}C^{\beta}$ s (12)
			1102			CH_3 r2 (51), $C^{\alpha}C^{\beta}$ s (12)
	1057 M				1064	$C^{\alpha}C^{\beta}$ s (26), CH_3 r1 (22), H^{α} b1 (19), CH_3 r2 (14)
		1063				$C^{\alpha}C^{\beta}$ s (57), H^{α} b1 (14), CH_3 r1 (11)
			1063			$C^{\alpha}C^{\beta}$ s (57), H^{α} b1 (14), CH_3 r1 (11)
				1063		$C^{\alpha}C^{\beta}$ s (26), CH_3 r1 (22), H^{α} b1 (19), CH_3 r2 (14)
	1020 VW				1009	ND ib (51), H^{α} b1 (10)
		1003				ND ib (35), CH_3 r1 (28), CH_3 r2 (11), NC^{α} s (10)
			995			CH_3 r1 (32), ND ib (29), NC^{α} s (13), $C^{\alpha}C$ s (12), CH_3 r2 (10)
	999 M			994		ND ib (56)
		940				CH_3 r1 (26), ND ib (19), NC^{α} s (18)
	942 M		936			ND ib (22), CH_3 r1 (21), NC^{α} s (15)

Table II (*Continued*)

observed[a]		calculated				
Raman	IR	A	B_1	B_2	B_3	potential energy distribution[b]
	917 VW			900		NC^{α} s (32), CH_3 r1 (22), CN s (15)
					897	NC^{α} s (36), CH_3 r1 (22), CN s (14)
		896				CN s (18), $C^{\alpha}C$ s (14), CO s (12), CNC^{α} d (11)
	888 W		883			CN s (20), $C^{\alpha}C$ s (13), CO s (13), CNC^{α} d (11), ND ib (11)
				841		$C^{\alpha}C$ s (33), NC^{α} s (15), $C^{\alpha}C^{\beta}$ s (12), CN s (10)
	843 M[e]				840	$C^{\alpha}C$ s (36), CN s (12), NC^{α} s (10), $C^{\alpha}C^{\beta}$ s (10)
					758	CO ib (21), $C^{\alpha}C$ s (13), NC^{α} s (13), CNC^{α} d (12), $NC^{\alpha}C$ d (12), C^{β} b2 (12)
	761 MW			756		CO ib (19), $C^{\alpha}C$ s (15), C^{β} b2 (14), CNC^{α} d (13), $NC^{\alpha}C$ d (12), NC^{α} s (12)
			685			CO ob (65), C^{β} b1 (15), H^{α} b1 (11)
		683				CO ob (65), C^{β} b1 (15), H^{α} b1 (11)
					635	CO ob (48), $C^{\alpha}CN$ d (19), C^{β} b2 (12)
	631 sh			633		CO ob (48), $C^{\alpha}CN$ d (17), C^{β} b2 (11)
		624				CO ib (53), $C^{\alpha}C$ s (15)
	626 MW		615			CO ib (55), $C^{\alpha}C$ s (14)
				592		CO ob (32), $C^{\alpha}CN$ d (28)
	599 MW				592	CO ob (34), $C^{\alpha}CN$ d (28)
		510				CN t (81), ND ob (26), ND···O t (13)
				510		CN t (67), ND ob (48), ND···O t (14)
	529 sh		506			CN t (79), ND ob (26), ND···O t (12)
	523 M				502	CN t (66), ND ob (50), ND···O t (14)
					445	C^{β} b1 (45), CN t (18)
	446 MW, br			443		C^{β} b1 (48), CN t (12)
		426				C^{β} b2 (73), ND ob (16), $NC^{\alpha}C$ d (12)
			427			C^{β} b2 (75), ND ob (16), $NC^{\alpha}C$ d (10)
			327			$NC^{\alpha}C$ d (29), $C^{\alpha}C$ s (10)
		324				$NC^{\alpha}C$ d (26), C^{β} b2 (12), $C^{\alpha}C$ s (10)
				285		CO ib (34), $NC^{\alpha}C$ d (21), CNC^{α} d (13), C^{β} b2 (13)
					284	CO ib (33), C^{β} b2 (21), $NC^{\alpha}C$ d (18), CNC^{α} d (11), C^{β} b1 (11)
			284			$C^{\alpha}CN$ d (38), $C^{\alpha}C^{\beta}$ t (20), D···O s (14)
		266				$C^{\alpha}CN$ d (35), $C^{\alpha}C^{\beta}$ t (35), $NC^{\alpha}C$ d (12)
				252		C^{β} b2 (51)
					250	C^{β} b2 (44)
				238		$C^{\alpha}C^{\beta}$ t (91)
					238	$C^{\alpha}C^{\beta}$ t (89)
			238			$C^{\alpha}C^{\beta}$ t (68)
		236				$C^{\alpha}C^{\beta}$ t (58), $NC^{\alpha}C$ d (13), $C^{\alpha}CN$ d (12)
			198			CNC^{α} d (46), D···O s (17), $C^{\alpha}C^{\beta}$ t (10)
		175				CNC^{α} d (66), $C^{\alpha}CN$ d (10)
					155	D···O s (60)
		139				ND ob (35), CO ob (19), NC^{α} s (12), $C^{\alpha}CN$ d (10), H^{α} b2 (10)
			137			ND ob (46), CO ob (18), NC^{α} s (14), H^{α} b2 (13), $C^{\alpha}CN$ d (10)
				115		CNC^{α} d (23), NC^{α} C d (16), $C^{\alpha}CN$ d (13), ND ob (12)
			105			C^{β} b1 (18), CN t (18), ND···O t (18)
					91	ND ob (27), D···O s (21), $C^{\alpha}C$ t (19), CNC^{α} d (14)
		90				C^{β} b1 (23), ND ob (22), D···O s (17), $C^{\alpha}C$ t (11)
					83	CN t (38), ND···O t (18), CO···D ib (17), ND ob (15), D···O s (12), NC^{α} t (11)
				71		D···O s (30), $C^{\alpha}C$ t (27), NC^{α} t (23), CN t (12), ND ob (10)
		37				ND···O ib (39), ND···O t (32), ND ob (22), D···O s (12), CO···D t (12)
			38			ND ob (64), ND···O ib (40), CN t (20)
				30		ND···O ib (62), CN t (42), ND ob (42), CO···D ib (18)
		19				ND ob (37), CO···D ib (24), CO···D t (22), H^{α}···H^{α} s (19), ND···O ib (12), ND···O t (12), CN t (11)

[a] S = strong, M = medium, W = weak, V = very, sh = shoulder, br = broad, ∥ = parallel dichroism, ⊥ = perpendicular dichroism. [b] s = stretch, as = antisymmetric stretch, ss = symmetric stretch, b = angle bend, ib = in-plane angle bend, ob = out-of-plane angle bend, ab = antisymmetric angle bend, sb = symmetric angle bend, r = rock, d = deformation, t = torsion. Only contributions 10% or greater are included. [c] Unperturbed frequency. [d] Value taken from ref 11. [e] Overlapped by carboxylate ion band.

modes (mainly CO stretch) are well predicted, as before,[2] and so is their slight downward shift on N-deuteration. The amide II modes (primarily NH in-plane bend plus some CN stretch) are similarly accounted for, as is their disappearance on deuteration. The consequent appearance of the CN stretch contribution at 1464 cm^{-1} is also well predicted. The 1402-cm^{-1} band is clearly seen to disappear on deuteration, requiring that it have some component of NH in-plane bend. Our present calculation shows this to be the case, which the previous one[2] did not, and correctly predicts the absence of this band in the spectrum of β-(Ala-ND)$_n$. Similarly, we would not predict deuteration shifts for the infrared bands at 1372 and 1386 cm^{-1} (which would be indicated by the earlier analysis[2]), and indeed none are observed, consistent with the absence of any NH in-plane bend contributions to these modes. Again, the 1335 R, 1330 IR bands are predicted to have large NH in-plane bend contributions, and the infrared band indeed disappears on N-deuteration. (We do not believe that the 1326-cm^{-1} band in β-(Ala-ND)$_n$ can be assigned to the same mode as the 1330-cm^{-1} band because the former is stronger and sharper; in any case its presence and altered character are predicted by the calculation.)

The so-called amide III modes (NH in-plane bend plus CN stretch) are now more clearly defined, once we no longer require the assignment of the 1240-cm^{-1} infrared band to the APPS structure[2] but associate it with a disordered component. The 1243-cm^{-1} Raman band is now assigned to an A species mode (vs. B_2/B_3 before[2]), and the 1226 R, 1222 IR bands can both be assigned to B_1 species modes. These are seen to contain about equal contributions of NH in-plane bend and CN stretch, although these two are by no means the major contributors to the mode, H^α bend and NC^α stretch being very important. The sensitivity of the amide III mode to side-chain composition has already been noted[2,14] as has the dependence of its character on chain conformation.[15] Here we also see that NH in-plane bend contributes to frequencies between the amide II and amide III modes, near 1400 and 1330 cm^{-1} in the present case.

The so-called amide V mode (associated with NH out-of-plane bend) is found to have almost no dichroism,[12] indicating that parallel (B_1) and perpendicular (B_3) bands occur at about the same frequency. Our present calculation reproduces this result much better than did the previous one[2] and also predicts that the 698 R band should be associated with these modes. It is interesting that NH out-of-plane bend also contributes to a mixed mode at 615 cm^{-1}, which is predicted to shift to ~634 cm^{-1} on N-deuteration. The observed 615-cm^{-1} band is indeed absent in the deuterated molecule, and a shoulder is observed at 631 cm^{-1}. The CO out-of-plane bend modes near 597 cm^{-1}, not observed in β-(Ala)$_n$, are present near their predicted values in β-(Ala-ND)$_n$. The predominant CO in-plane bend mode observed at 629 cm^{-1} in the infrared is found at 626 cm^{-1} in the N-deuterated molecule, consistent with the slight frequency drop predicted by the calculation.

In the present refinement we have also taken greater care to refine the CH_3 symmetric bend modes so that they appear predominantly in the ~1370–1380-cm^{-1} region, where they are expected as relatively pure group frequencies. This is now the case, and these bands are not expected to, and do not, shift on N-deuteration, in contrast to our previous calculation.[2]

In addition to the above predictions, other results for the N-deuterated molecule are in good accord with assignments in the hydrogenated molecule. Thus, a band at 1306 cm^{-1} retains much of the character (H^α bend) that it had in β-(Ala)$_n$. The weak band at 1190 cm^{-1} may appear as a result of the loss of NH in-plane bend contribution in the (unobserved) 1196-cm^{-1} mode of β-(Ala)$_n$. Assignments of observed bands at 1207 and 1142 cm^{-1} in β-(Ala-ND)$_n$, although in good agreement with calculated frequencies, are nevertheless somewhat uncertain because of the presence of strong CF_3 bands at these frequencies arising from CF_3COO^- ions[16] in our KBr pellets. The 1057-cm^{-1} band has retained the character that its counterpart at 1052 cm^{-1} has in β-(Ala)$_n$. The contribution of ND in-plane bend to a wide range of bands is very well accounted for: a possible observed band at 1142 cm^{-1} (uncertain because of an overlapped CF_3 mode) has a small ND in-plane bend component and could derive from a mode of otherwise similar character found at 1120 cm^{-1} in β-(Ala)$_n$; a new band is found at 1020 cm^{-1}, in a region where nothing is observed or predicted in the parent molecule, and this corresponds fairly well with a predicted mainly ND in-plane bend mode; the 999-cm^{-1} band, if it is associated with the B_1 species mode, contains a significant ND in-plane bend component but is otherwise similar to the strong 966-cm^{-1} B_1 mode of β-(Ala)$_n$, thus accounting for the ~30-cm^{-1} shift in the latter frequency (of course, the B_2 ND in-plane bend mode may also be contributing at 999 cm^{-1}); a new band is found at 942 cm^{-1}, which is predicted near this frequency as a mode with significant ND in-plane bend character; and the 888-cm^{-1} B_1 species mode, with a modest ND in-plane bend contribution, is clearly correlatable with the 902-cm^{-1} B_1 mode of β-(Ala)$_n$, which (despite the absence of any NH in-plane bend component) otherwise is of generally similar character. These results emphasize how wide ranging is the influence of substituting ND for NH, even on skeletal-type modes. Other bands that retain their essential character on N-deuteration, and whose frequencies are reasonably well predicted, are those at 925 (917 in β-(Ala-ND)$_n$), 837 (843), and 778 (761) cm^{-1}. The new bands near 523 cm^{-1} are clearly assignable to ND out-of-plane modes, although the frequency agreement is poor (possibly due to anharmonicity effects). In summary, considering that the frequencies of β-(Ala-ND)$_n$ were not used in refining the force field, we feel that the present force field for β-(Ala)$_n$ (which gives an average discrepancy of 4.6 cm^{-1} between observed and calculated frequencies in the range of 90–1700 cm^{-1}) provides a very satisfactory description of the normal vibrations of this molecule and its N-deuterated derivative.

It is also of interest to note that the unperturbed ND stretch frequency, as probably given by a three-level Fermi resonance analysis,[17] is higher than the calculated value by the same amount as for (Gly I)$_n$,[1] viz., about 50 cm^{-1}. The interacting combination bands, in distinction to the (Gly I)$_n$ case,[1] are found to be higher than the unperturbed ND stretch mode but are similar in nature to those found in (Gly I)$_n$.[17] The spectroscopic indication that there is a stronger hydrogen bond, both in the normal and in the deuterated molecules, is consistent with the shorter N···O distance in the APPS structure of β-(Ala)$_n$ (2.73 Å) as compared to the APRS structure of (Gly I)$_n$ (2.91 Å).

Since the β-(Ala)$_n$ force field was refined so as to achieve maximum transferability from that of (Gly I)$_n$,[1] it is of interest to compare these two force fields. Of the 100 force constants in Table I that do not involve transition dipole coupling, 51 are identical with those in the (Gly I)$_n$ force field, 16 are different (2 are zero and therefore are not included in Table I), and 35 represent the new force constants associated with the CH_3 side chain. In Table III we compare these 16 force constants in the (Gly I)$_n$ and β-(Ala)$_n$ force fields. (The $f(H^\alpha \cdots H^\alpha)$ force constant was kept the same even though the $H^\alpha \cdots H^\alpha$ distances are different because we have no basis for refining it other than

Table III
Comparison of Nonequal Force Constants for Poly(glycine I) and β-Poly(L-alanine)

force constant	$(Gly\ I)_n$	β-$(Ala)_n$
$f(NC^{\alpha})$	5.043	4.523
$f(C^{\alpha}C)$	4.409	4.160
$f(NH)$	5.840	5.674
$f(C^{\alpha}H^{\alpha})$	4.564	4.4628
$f(H\cdots O)$	0.125	0.150
$f(C^{\alpha}CN)$	1.400	1.033
$f(CNC^{\alpha})$	0.687	0.5259
$f(NC^{\alpha}H^{\alpha})$	0.715	0.765
$f(NC^{\alpha},NC^{\alpha}H^{\alpha})$	0.517	0.627
$f(CO,C^{\alpha}CN)$	−0.150	0.000
$f(CNC^{\alpha},NC^{\alpha}H^{\alpha})$	0.000	0.100
$f(CNC^{\alpha},C^{\alpha}NH)$	−0.040	0.000
$f(C^{\alpha}NH,CNH)$	0.0065	0.038
$f(CC^{\alpha}H^{\alpha},CO\ ob)$	0.100	0.150
$f(NH\cdots O\ ib,NH\ ob)$	0.000	−0.039
$f(NH\ ob,CN\ t)$	−0.1677	−0.1477

the lowest frequency A species mode, which has not yet been observed. In $(Gly\ I)_n$ this force constant determines the splitting between infrared- and Raman-active CH_2 bending modes.) The changes in $f(NH)$ and $f(H\cdots O)$ are obviously necessitated by the difference in hydrogen bond strength between the two structures. The changes in the other force constants are undoubtedly due mainly to the presence of the CH_3 side chain but probably also to the small differences in backbone angles between $(Gly\ I)_n$ and β-$(Ala)_n$. In any case, these force constants are related mainly to the C^{α} atom, which is not surprising in terms of the influence of the side chain on the local charge distribution. This effect is also manifested by the significant mixing of side-chain modes (CH_3 rock, $C^{\alpha}C^{\beta}$ stretch, C^{β} bend, and $C^{\alpha}C^{\beta}$ torsion) with backbone modes, a situation which is not as true in the case of $(Gly\ I)_n$. Thus, $(Ala)_n$ should serve as a better model for the vibrations of the polypeptide chain in proteins.

Conclusions

The availability of the spectrum of β-$(Ala\text{-}ND)_n$, as well as an improved transferable force field for $(Gly\ I)_n$,[1] has enabled us to achieve a significant improvement in the force field and band assignments for APPS $(Ala)_n$. This now provides a more secure basis for the vibrational analysis of other polypeptide chain structures as well as for the development of an approximate force field[3] for the calculation of the normal modes of larger molecules.

Acknowledgment. This research was supported by National Science Foundation Grants PCM-7921652 and DMR-7800753. A.M.D. expresses appreciation to the Macromolecular Research Center for fellowship support.

References and Notes

(1) Dwivedi, A. M.; Krimm, S. *Macromolecules*, preceding paper in this issue.
(2) Moore, W. H.; Krimm, S. *Biopolymers* **1976**, *15*, 2465.
(3) Dwivedi, A. M.; Krimm, S., to be published.
(4) Arnott, S.; Dover, S. D.; Elliott, A. *J. Mol. Biol.* **1967**, *30*, 201.
(5) Colonna-Cesari, F.; Premilat, S.; Lotz, B. *J. Mol. Biol.* **1974**, *87*, 181.
(6) Moore, W. H.; Krimm, S. *Biopolymers* **1976**, *15*, 2439.
(7) Krimm, S.; Abe, Y. *Proc. Natl. Acad. Sci. U.S.A.* **1972**, *69*, 2788.
(8) Moore, W. H.; Krimm, S. *Proc. Natl. Acad. Sci. U.S.A.* **1975**, *72*, 4933.
(9) Fanconi, B. *Biopolymers* **1973**, *12*, 2759.
(10) Frushour, B. G.; Koenig, J. L. *Biopolymers* **1974**, *13*, 455.
(11) Elliott, A. *Proc. R. Soc. London, Ser. A* **1954**, *226*, 408.
(12) Itoh, K.; Nakahara, T.; Shimanouchi, T.; Oya, M.; Uno, K.; Iwakura, Y. *Biopolymers* **1968**, *6*, 1759.
(13) Frushour, B. G.; Painter, P. C.; Koenig, J. L. *J. Macromol. Sci., Rev. Macromol. Chem.* **1976**, *C15*, 29.
(14) Hsu, S. L.; Moore, W. H.; Krimm, S. *Biopolymers* **1976**, *15*, 1513.
(15) Krimm, S.; Bandekar, J. *Biopolymers* **1980**, *19*, 1.
(16) Pouchert, C. J. "The Aldrich Library of Infrared Spectra"; Aldrich Chemical Co.: Milwaukee, Wisc., spectrum no. 294C.
(17) Krimm, S.; Dwivedi, A. M. *J. Raman Spectrosc.*, in press.

Light Scattering Studies on the Morphology and Deformation Mechanism of Poly(tetramethylene oxide)–Poly(tetramethylene terephthalate) Block Polymer[1]

Masaru Matsuo,* Keiko Geshi, Akiyo Moriyama, and Chie Sawatari

Department of Clothing Science, Faculty of Home Economics, Nara Women's University, Nara 630, Japan. *Received August 5, 1980*

ABSTRACT: The morphology and deformation mechanism in poly(tetramethylene oxide)–poly(tetramethylene terephthalate) block polymers were studied by small-angle light scattering, polarized microscopy, and birefringence experiments. A series of experiments was carried out using specimens with a relatively high concentration of soft rubbery segments. On the basis of the experimental results, two models were proposed in terms of the morphology and the deformation mechanism of the spherulitic texture. The H_v light scattering patterns were theoretically calculated for the two models. One of them is associated with an orientation disorder of rodlike lamellae with respect to the spherulitic radius, and the other with an affine deformation mode of a perfect spherulite. The patterns observed were well accounted for by the results calculated.

I. Introduction

There have been several reports[2-7] on the morphology and deformation of segmented polymers synthesized by combining blocks or segments of two dissimilar homopolymers to form a polymer chain, in which one component is characterized as a rubbery or soft segment with a relatively low glass transition temperature and the other as a hard segment with a glassy-amorphous or semicrystalline nature. There is currently considerable interest in the fine-structure and physical properties of these polymers. The morphology of diblock and triblock copolymers made from styrene and isoprene cast from several solvents has been shown to consist of spheres, rods, or sheets of one component dispersed in a continuous matrix of the other.[8-11]

Kawai et al.[3] studied the morphology and deformation mechanism of spherulitic textures in segmented poly(urethaneureas). They concluded that the observed orien-

0024-9297/82/2215-0193$01.25/0 © 1982 American Chemical Society